Design of an Air-Cooled Metallic High-Temperature Radial Turbine

Philip H. Snyder*
General Motors Corporation, Indianapolis, Indiana
and
Richard J. Roelke†
NASA Lewis Research Center, Cleveland, Ohio

Recent trends in small advanced gas turbine engines call for higher turbine inlet temperatures. Advances in radial turbine technology have opened the way for a cooled metallic radial turbine capable of withstanding turbine inlet temperature of 2500°F while meeting the challenge of high efficiency in this small flow size range. In response to this need a small air-cooled radial turbine has been designed utilizing internal blade coolant passages. The coolant flow passage design is uniquely tailored to simultaneously meet rotor cooling needs and rotor fabrication constraints. The rotor flow-path design seeks to realize improved aerodynamic blade loading characteristics and high efficiency while satisfying rotor life requirements.

Introduction

REQUIREMENTS for advanced turbine engines call for increased specific power and improved specific fuel consumption (SFC). Results of basic gas turbine cycle studies have generally shown that these requirements can be met through the use of increased turbine inlet temperatures and increased cycle pressure ratios. The result is a significant reduction in core equivalent mass flow rates and a commensurate reduction in core flow passage widths. For axial turbines, small passage widths are associated with low-aspect ratio airfoils giving rise to secondary flow losses and increased tip clearances, both of which reduce stage efficiencies. Past studies have shown that radial turbines offer lower sensitivity to the efficiency penalties of reduced passage widths and, hence, result in designs with higher turbine efficiencies at low equivalent flow values. In addition, radial turbines offer the potential of high loading per stage. This gives rise to the possible reduction in number of stages, which can result in cost benefits. The use of a radial turbine in the gasifier section thus becomes attractive in the design of small turbine engines.

The development of high-temperature capabilities in radial turbines has recently been pursued via ceramic blading. However, prior to the development of a mature ceramic radial turbine technology, use of the air-cooled metallic radial turbine had been proposed for advanced engines with high power-to-weight and improved SFC requirements.

The objective of this paper is to review briefly recent advances in cooled radial turbine technology and to present work recently completed on the design of an air-cooled radial turbine. Operation of the turbine was targeted for a turbine inlet temperature of 2300°F and a cycle pressure ratio of 14:1 with rotor flow of 4.6 lbm/s. Design goals were high aerodynamic performance ($\eta_{TT} < 86\%$), a rotor life of 5000 h and 6000 cycles, and the utilization of fabrication capabilities and material properties available within the next 10 years.

Presented as Paper 88-2872 at the AIAA/ASME/SAE/ASEE 24th Joint Propulsion Conference, Boston, MA, July 11-13, 1988; received Sept. 20, 1988; revision received March 2, 1989.

*Development Engineer, Allison Gas Turbine Division.
†Aerospace Engineer, Propulsion Systems Division.

Advances in Radial Turbine Design

A number of efforts have built upon the radial turbine technology base laid down by application of the radial turbine in automotive and auxiliary power unit (APU) turbine engines. This work has made significant advances in overcoming some perceived difficulties in cooled radial turbine application. Areas of difficulty include packaging, rotor stress and life, aerodynamic efficiency, and cooled rotor fabrication.

Packaging

Packaging of the radial turbine has been enhanced when combined with a reverse flow or "foldback" annular combustor design as shown in Fig. 1.[1] Compactness is achieved through combination of the turning region downstream of the combustor with the nozzle row. The placement of an axial power turbine stage following the radial gasifier stage has been successfully demonstrated and can exhibit high efficiencies in a close-coupled design.[2,3] Radial turbines also prove advantageous in packaging the nonconcentric configuration, presented in Fig. 2, where interspool flow paths are conducive for use with scroll technology, combining well with radial turbine nozzle design.[1]

Rotor Life

Previous research has shown that in the design of a high-temperature radial turbine, the single most critical parameter limiting radial turbine performance is allowable rotor stress. Previous work resulting in the successful design and test of a dual-alloy radial turbine rotor has significantly aided in alleviating this constraint. This work was conducted as part of a program demonstrating high-temperature radial turbine technology.[4-6] Until that time rotor stresses severely limited achievable tip speeds to nonoptimal levels in terms of maximizing turbine efficiencies. Excessive bore stresses had precluded their feasibility, particularly in the presence of front-drive power turbine shafting, which caused sizable bore holes.

As part of this previous program, radial turbine rotors were fabricated utilizing separate hub and blade shell pieces bonded together using the hot isostatic pressure-bonded (HIP-bonded) process. This approach permitted the selection of optimal materials for both the hub piece and the blades and also permitted the casting of the blade shell as an integral piece with hollow, air-cooled blades. The design approach selected for the turbine utilized a cast Mar-M247 air-cooled airfoil shell HIP-bonded to a PA101 powder metal hub. This program

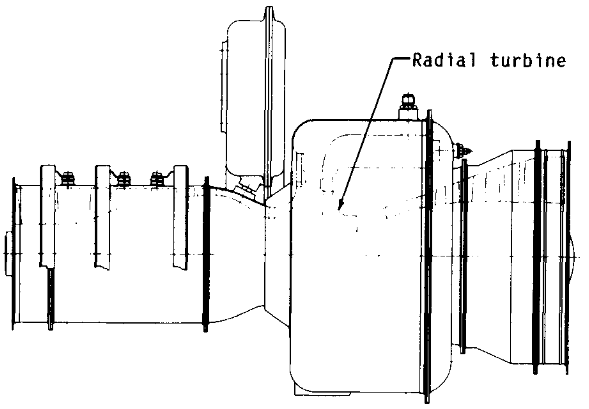

Fig. 1 Concentric engine outline.[1]

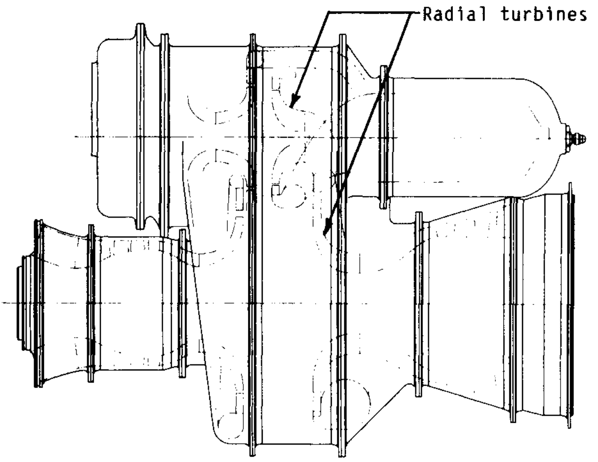

Fig. 2 Nonconcentric engine outline.[1]

demonstrated the required manufacturing processes and resulted in the fabrication of complete rotor assemblies whose mechanical integrity and life were verified by testing.

Radial Turbine Efficiency

With proper speed matching, now made possible with improvements in rotor life, radial turbines have demonstrated efficiencies in excess of 90%.[7] The way to further improvements, particularly for highly loaded designs, has recently been explored analytically through development of improved blade design and flow-path contouring investigations.[8-10] Estimates of current and goal technology for radial turbine performance in the year 2000 are shown in Fig. 3. In addition, radial turbines have also shown superiority to axial turbines in their ability to incorporate variable capacity. The benefit stems partly from the inherent two-dimensionality of the radial turbine's nozzle row blading, which significantly aids the application of variable geometry to the radial turbine stage. The movable sidewall concept shows particular promise in its ability to maintain efficiency at part capacity.[11-13]

Radial Turbine Cooling

The addition of cooling to the blades of a metal radial turbine has provided a significant challenge. Initial concepts and trials have been published detailing cooled metal rotor design approaches including investment casting, lamination construction, bicasting, split-blade HIP bonding, and dual-alloy HIP-bonded rotor fabrication.[14-19] The investment cast and HIP-bonded approach developed as part of the previous Army-Funded work has demonstrated the greatest promise in

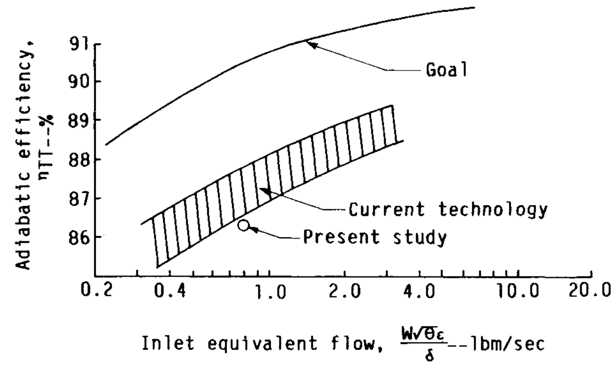

Fig. 3 Current technology and goal radial turbine performance.

meeting coolant passage constraints while yielding rotors that demonstrate adequate life. The study presented here adds to this design approach by developing a second-generation investment cast and HIP-bonded cooled metal rotor design that is suitable for commercial fabrication and promises acceptable efficiency and rotor life. The design builds upon the work conducted for the Army. The current study seeks to enhance rotor aerodynamics, further improve cooling performance, and furnish the test rotors necessary to provide definitive information on cooling a high-temperature radial turbine rotor.

Rotor Aerodynamic Design

Table 1 presents design point values for the radial turbine. The design reflects selection of the operating point within the optimal range in terms of specific speed and blade-jet speed ratio. Average exit swirl values were set to zero for design point operation. The design does not attempt to be fully optimal and reflects limitations imposed by rig hardware design constraints. Development of a radial turbine that takes full advantage of increased design capabilities awaits application in a suitable engine program.

Detailed aerodynamic design of the rotor was accomplished using two- and three-dimensional inviscid codes in conjunction with one-dimensional boundary-layer analyses. For the purpose of this study the shroud contour and inducer width were predetermined for conformance to NASA rig hardware constraints. Blade angle distribution and hub contour are design parameters subject to selection in providing the desired blade loading distributions.

The logarithmic blade thickness distributions used were based strongly on previous HTRT optimization studies. Blade angle distribution was selected to achieve nearly constant aerodynamic loading on the blade for the mean and shroud contours with minimal turning downstream of the rotor throat. Distributions of this type load the blade uniformly over its length and avoid diffusion on blade suction surfaces. The resulting surface velocity distributions for the rotor are shown in Fig. 4. Note that for the hub streamline an excessive

Table 1 Turbine design point conditions

Rotor inlet total temperature, °F	2300
Vane inlet total pressure, psia	200
Total-to-total expansion ratio	3.66
Actual flow, lbm/s	4.56
Equivalent flow, llb/s	0.80
Power output, hp	1191
Corrected work, $\Delta H/\theta_c$	34.9
Mechanical speed, rpm	61,900
Rotor diameter, in.	8.02
Rotor tip speed, ft/s	2166
Specific speed, rpm/ft$^{3/4}$s$^{1/2}$	62.2
Blade-jet speed ratio	0.66
Adiabatic efficiency, T-to-T, %	86.0

amount of diffusion was present over a significant portion of the blade. This was partly the result of specification of radial filament blading for the rotor as is common in radial turbine design practice. Radial filament blading eliminates bending stresses in the blade caused by rotational forces and thus reduces overall blade stresses.

One-dimensional boundary-layer analysis indicated the likelihood of boundary-layer separation near the intersection of the hub and blade suction surfaces. To avoid this loss-producing mechanism, the alternative hub contours of Fig. 5 were examined for their potential to reduce the degree of diffusion. Results indicated that separation can be delayed or eliminated as illustrated in Fig. 6. Alterations to the mean and shroud streamline loadings with this hub contouring were insignificant. However, the study showed that the impact on rotor and blade stress caused by this modification can be significant. Although blade stresses generally decrease with shortened blades, the potential exists for hub stresses to rise. Thus, the addition of significant material to the hub, as in contour B, calls for a comprehensive re-evaluation of the blade/hub stress picture tradeoffs. This analysis was beyond the scope of the study. For the purpose of this study the hub diffusion offered by contour A was sufficiently improved over that of the baseline to warrant incorporation into the final rotor design.

Coolant Passage Design

As part of the previously funded cooled radial turbine effort, a highly instrumented engine scale rotor was tested under warm turbine test conditions to evaluate its cooling performance. Based on this work, the need for improvements in internal airfoil coolant passage design was identified as a next step in developing a cooled high-temperature radial turbine fully meeting the requirements of advanced technology engines. A thorough consideration of coolant flow-path design constraints was found to be most important in achieving a successful design.

Coolant Passage Design Constraints

Design of the coolant passages within the blade is constrained by three considerations: 1) blade internal heat transfer, 2) coolant flow pressure losses, and 3) compatibility with fabrication methods. Fabrication constraints, by far the most restrictive of the three constraints, are so limiting that the design process, to a high degree, revolves around the limits placed on coolant passage geometry. A brief description of the manufacturing process illustrates the impact of these constraining factors.

Fabrication is accomplished by the investment casting process in which a wax replica of the finished rotor blade shell is produced. A core is placed within the blades of this wax replica. This core, constructed of ceramic within the blades of this wax replica. This core, constructed of ceramic material, occupies the volume to become the coolant passageway. In the casting process a mold is made around this wax replica with the core material secured to the mold via protrusions through the (wax) blade shell. The wax is removed by heat, and the resulting mold is used in the casting process. The survival of the ceramic core during this process is key to producing a blade shell meeting the design requirements. Upon successful casting the ceramic material is removed from the metal shell by chemical leaching, resulting in a hollow blade shell casting complete with integral coolant passages.

Figures 7 illustrates the successfully fabricated coolant flow passageway of the previous program. A major feature of this design was the flow split between the inducer-directed coolant flow and the flow directed to the hub section of the blade. This split resulted in an inherent uncertainty as to actual distribution of coolant flow within the blade. This uncertainty is due in part to the lack of appropriate means of adequately inspecting the internal sturcture of the final cast shell. Additional uncertainty arises in modeling the complexities of the coolant flow-path pressure loss characteristics in the presence of rotational forces set up within the blade. Uncertainties about the magnitude of coolant flow within the blade inducer region gave rise to difficulties in interpreting heat-transfer data received from testing this rotor.

Fabrication of this rotor was, however, highly successful. Features of this design that contributed to its success were the position of the flow inlet on the rotor back face, the pressure side discharge arrangement, and the internal tie between cool-

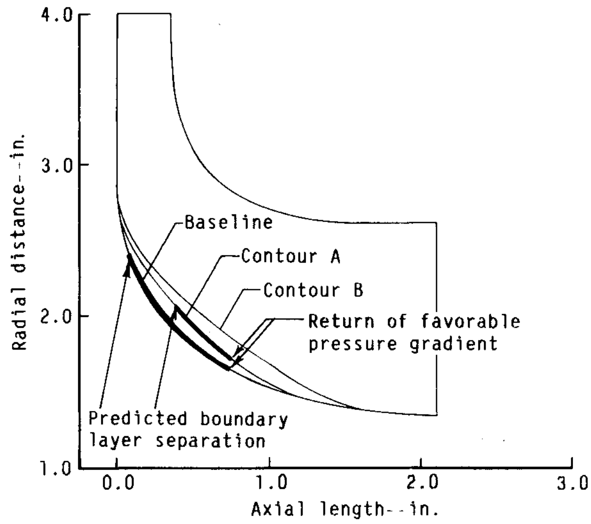

Fig. 5 Alternate hub contour for improved rotor blade diffusion characteristics.

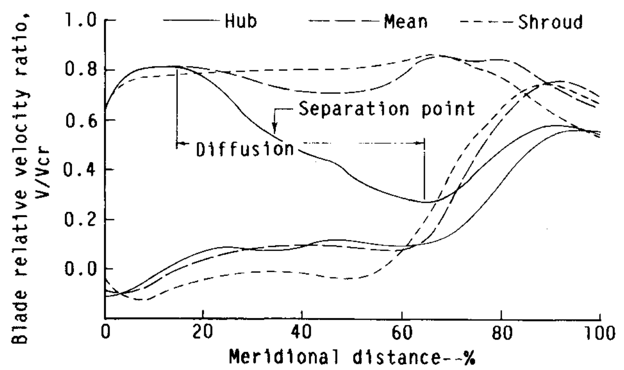

Fig. 4 Predicted blade relative velocity for baseline rotor hub contour.

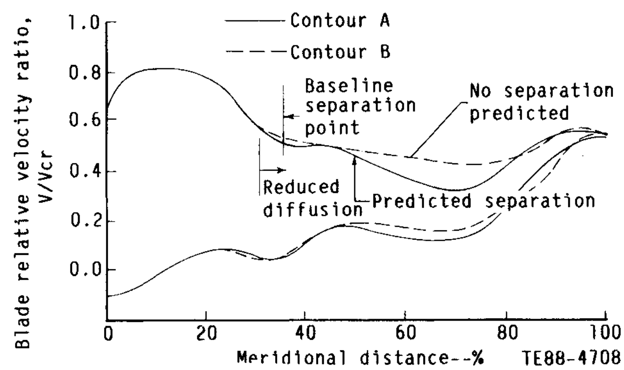

Fig. 6 Improved hub streamline surface velocity profiles with hub contouring.

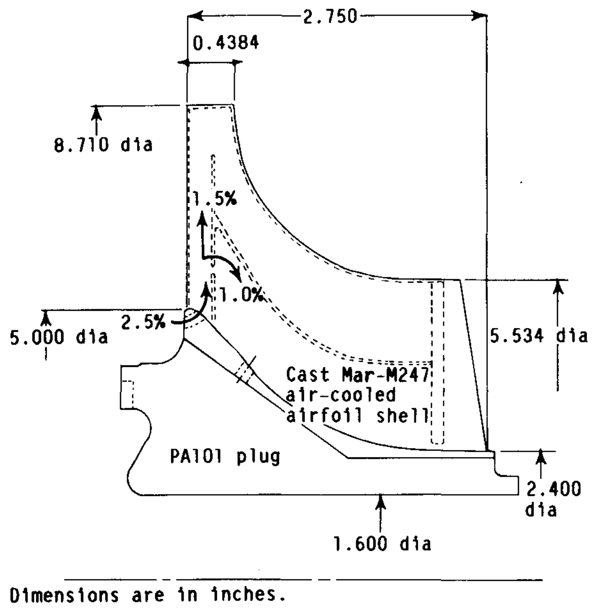

Fig. 7 Cooled rotor design developed under contract DDAJ02-77-C-0031.[4]

ant passages at the flow split position. Also important to this program was the capability of securing the core during the fabrication process via protrusions through the shell at the inducer tip and the hub sections. Both openings are later closed by a braze process on the final rotor.

Fabrication constraints that limit the allowable core passage geometries generally are based on previous casting experience. A summary of these constraints follows: 1) minimum core cross-sectional area (0.040 in.^{2}), 2) maximum length of unsupported core section (dependent on thickness of section), 3) minimum core and wall metal thicknesses (0.020 in.), and 4) minimum pin fin diameter (0.040 in.). These criteria apply specifically to a nominal 8-in.-diam rotor. Heat-transfer considerations in general call for complete coverage of the blade surface with adequate combinations of flow velocity, passage width, and wall surface roughness treatment. Coolant flow pressure loss is limited by available coolant pressures from compressor bleed and the position at which the coolant air is discharged. Mutual satisfaction of these considerations results in a successful design.

Selection of Coolant Passageway Configuration

The design process consisted of selecting cooling concepts, ranking concepts according to compatibility with the established constraints, examining the ability of each to perform the required cooling, selecting the final conceptual scheme, and finally determining the detailed coolant flow-path design.[20] Figure 8 presents concepts initially examined along with perceived benefits and deficiencies. Because of the goal of the program to produce a rotor capable of heat-transfer testing under well-defined conditions, the benefit of producing a design with well-defined internal flow characteristics was emphasized.

Figure 9 presents the resulting concept used for the detailed design effort. Of key importance to this concept was eliminating the branching coolant flow within the important inducer section. However, branching was required within the exducer section to achieve an even distribution of coolant air discharge, thus providing cooling to the trailing-edge region. Constraints on minimum wall and core thickness preclude the use of trailing-edge injection without excessively thickened blade trailing edges. Thick trailing edges result in excessive turbine efficiency penalties due to high flow blockage.

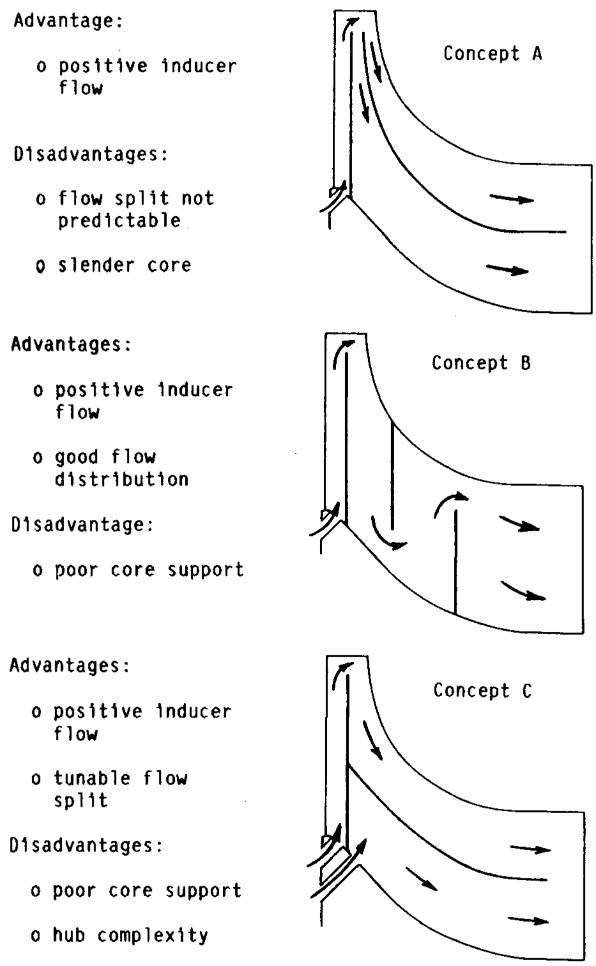

Fig. 8 Initial rotor coolant passage concepts.

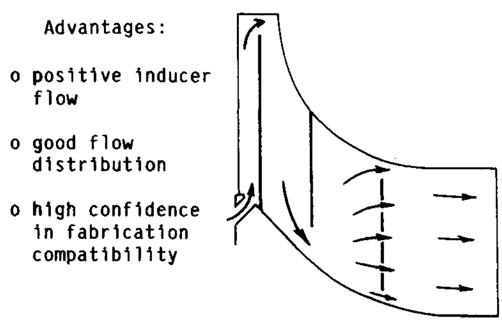

Fig. 9 Selected coolant flow-path concept.

Detailed Coolant Flow Path Design

Design of the detailed area distribution and branching coolant flow circuitry was accomplished using a detailed internal coolant flow model. The method utilizes flow modeling within the blade passages via discreet elements that include frictional and bend losses, branching losses, and "pumping effects" (changes in pressure due to fluid movement within the rotating passage). Temperature changes due to both heat-transfer and rotational effects are similarly modeled. Coolant flow preswirling (tangential onboard injection) is also modeled.

Results of the analysis demonstrated that pumping effects are extremely influential within the flow path. Thus, to achieve a uniform distribution of coolant air at the discharge, the circuitry of Fig. 10 was devised. The placement and

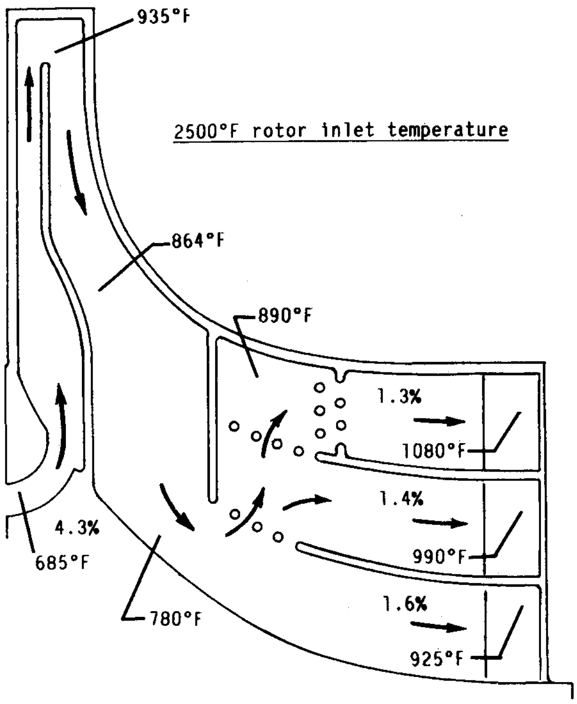

Fig. 10 Final internal blade coolant passageway design.

dimensions of the pin fins within the coolant passage were selected to provide a well-defined flow resistance in the radially outward direction to counter the pumping effect. The pumping force tends to drive the flow radially outward to the outermost coolant slot. The use of choked flow at the discharge point is not feasible in this case due to the minimum core size constraint. The series nature of the resistance is designed to provide a cumulative resistance with increasing radius to counter the cumulative effects of rotation.

An additional benefit is derived by selecting a design in which the entire coolant flow is routed through the rotor tip region. The design results in coolant passage tip region flow velocities giving high convective heat-transfer coefficients. This eliminates the need for the geometric complexity of heat-transfer enhancement through the use of discreet wall roughness.

The effects of blade rotation are also shown in Fig. 10. These forces cause significant compressions and expansions of the coolant flow with change in radius. The effects are sufficient to result in predicted temperature decreases in the bulk coolant flow for radially inward legs even though the fluid continues to pick up heat. Final design of the coolant flow path and required rates of coolant airflow were determined by an iterative process involving heat-transfer analyses to be described.

Representations of slices of the blade showing final coolant passage width distributions are shown in Fig. 11. The trailing-edge discharge configuration selected closely follows cooled-vane design technology and minimizes blade trailing-edge thickness. Blade angle distributions shown are the result of the comprehensive rotor aerodynamic design previously described. Cooling flow exiting the blade was not considered in the rotor aerodynamic design.

Heat-Transfer and Stress Analysis Results

As part of the detailed design process, two- and quasi-three-dimensional finite-element heat-transfer and stress analyses were made of the engine rotor concept. Coolant flow values and coolant passage geometry were selected to provide acceptable temperatures and material strengths within the dual-property rotor to meet rotor life requirements.

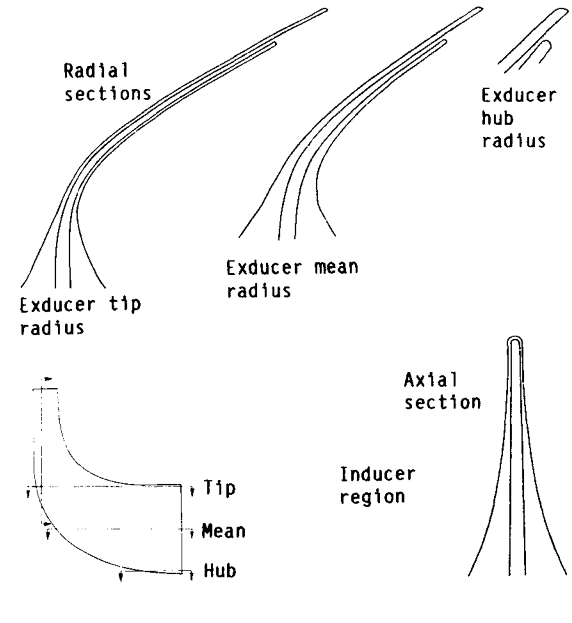

Fig. 11 Blade sections illustrating coolant flow-path design.

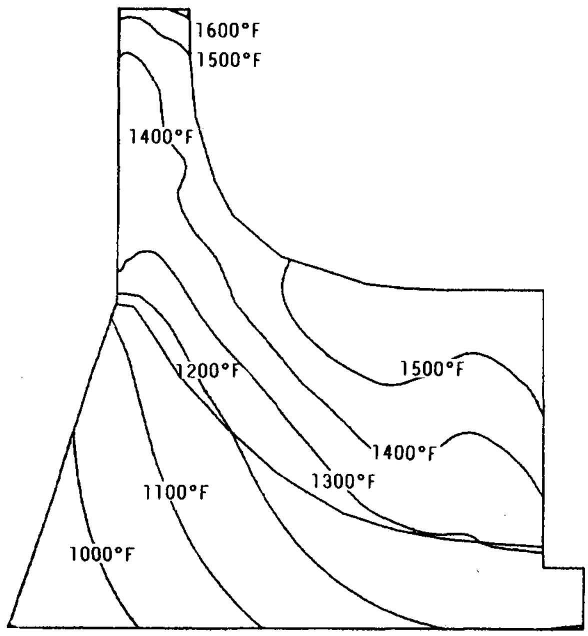

Fig. 12 Steady-state two-dimensional heat-transfer results, 2500°F rotor inlet temperature.

Heat-Transfer Results

In addition to a comprehensive analysis of the rotor design at 2300°F (program requirements), heat-transfer calculations evaluating design feasibility at 2500°F were completed. Results of the two-dimensional heat-transfer analysis are shown in Fig. 12. Rotor internal blade cooling was set at 4.3% of rotor inlet flow. In addition, a 1% hub film cooling and a 0.5% bore cooling were included. A significant feature of these heat-transfer results is the uniformity of blade temperatures, with a peak value of 1640°F, adequate for the Mar-M247 material in the tip region. Peak temperatures within the PA101 material are in the 1260°F range, ensuring retainment of suitable material properties within the hub. Thermal gradients within the hub are relatively low, giving rise to low steady-state thermal stresses in the hub.

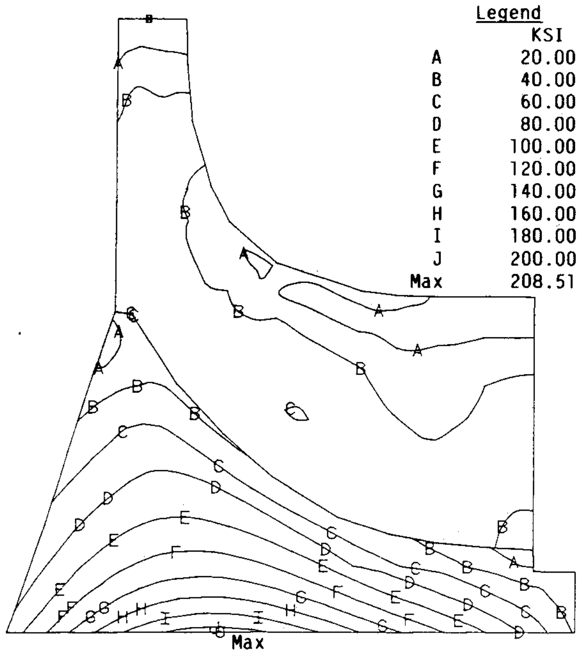

Fig. 13 Transient equivalent stress predictions.

Table 2 Summary of stress analysis results

Criteria (3σ)	Requirement	Computed
0.2 creep, h	1,000[a]	1,900
Burst speed, rpm	71,300 (130%)	79,300
LCF, cycles	6,000	6,367
Vibration, engine order	>4th	5.0

[a]5000-h life, 20% at design conditions.

Stress Analysis Results

Determination of low cycle fatigue (LCF) life is of prime concern for a radial turbine rotor, particularly with a center bore hole. LCF life assessment was made by modeling transient heat-transfer performance of the rotor during the period of acceleration from idle to design point conditions. Results for the time interval giving rise to maximum thermal gradients within the rotor serve as input to the stress analysis. Stress modeling based on these results is shown in Fig. 13. As expected, maximum stresses existed at the hub bore. Results of the complete stress analysis are summarized in Table 2. The results show that the rotor exceeds all life requirements based on anticipated 10-year advances in metal technology.

Conclusions

An advanced air-cooled metal rotor has been designed. A combination of series and parallel branched internal flow channels carrying a coolant airflow of 4.3% adequately cools the rotor for an inlet temperature of 2500°F. All fabrication limitations were considered in developing the successful design. Predicted rotor aerodynamics were enhanced through tailoring of blade angle distribution and hub contour shape to achieve improved blade loading distributions at the hub, mean, and shroud streamline positions.

Heat-transfer and stress examinations indicate that the resulting design of the cooled metal radial turbine rotor is capable of meeting all rotor life and efficiency requirements. Hence, the design of a cooled metallic radial turbine capable of operation at rotor inlet temperatures of 2500°F has been successfully completed.

The rotor is compatible with the requirements of an advanced turbine engine with a 14:1 compressor pressure ratio and a 2500°F rotor inlet temperature. Further effort shows promise in improving turbine efficiency through the comprehensive study of hub contour modification. Modification should be driven by aerodynamic performance improvement and developed in conjunction with heat-transfer and stress optimization analyses.

Acknowledgments

This work was funded by NASA through Contract NAS3-24230 and performed for the Army under Contract DDAJ02-77-C-0031. The authors wish to recognize the valuable contribution of D. L. Tipton, both in program supervision and technical guidance, and A. F. Ahles, D. W. Fox, D. B. Barnes, G. L. Vonnegut, and K. A. Green for their contributions to the heat-transfer, stress, and manufacturing process analyses, respectively.

References

[1]Larkin, T. R., "Small Engine Component Technology (SECT) Study Final Report," NASA CR-175081, U.S. Army Aviation Systems Command, Moffett Field, CA, AVSCOM-TR-86-C-8, March 1986.

[2]Rodgers, C., and Geiser, R., "Performance of a High-Efficiency Radial/AxialTurbine," American Society of Mechanical Engineers, New York, ASME Paper 86-GT-18, 1986.

[3]Kidwell, J. R., and Large, G. D., "Advanced Technology Components for Model GTP305-2 Aircraft Auxiliary Power System," Air Force Aero Propulsion Lab., Wright-Patterson AFB, OH, AFAPL-TR-79-2106, July 1979.

[4]Monson, D. S., and Ewing, B. A., "High-Temperature Radial Turbine Demonstration," U.S. Army Research and Technology Lab., Fort Eustis, VA, USAAVRADCOM-TR-80-D-6, April 1980.

[5]Ewing, B. A., Monson, D. S., and Lane, J. M., "US Army/Detroit Diesel Allison High-Temperature Radial Turbine Demonstration," AIAA Paper 80-0301, Jan. 1980.

[6]Tipton, D. L., and Monson, D. S., "High-Temperature Radial Turbine Aerodynamic Test," U. S. Army Research and Technology Lab., Fort Eustis, VA, USAAVRADCOM-TR-81-D-19, July 1981.

[7]Tipton, D. L., and McKain, T. F., "AGT 100 Turbomachinery," AIAA Paper 82-1207, June 1982.

[8]Perdichizzi, A., and Lozza, G., "Design Criteria and Efficiency Prediction for Radial In Flow Turbines," American Society of Mechanical Engineers, New York, ASME Paper 87-GT-231, 1987.

[9]Ribaud, Y., and Mischel, C., "Study and Experiments of a Small Radial Turbine for Auxiliary Power Units," American Society of Mechanical Engineers, New York, ASME Paper 86-GT-23, 1986.

[10]Civinskas, R. C., "Application of a Quasi-3D Inviscid Flow and Boundary Layer Analysis of the Hub-Shroud Contouring of a Radial Turbine," AIAA Paper 84-1297, 1984.

[11]Rogo, C., and Holbrook, M. R., "Cooled Variable Nozzle Radial Turbine for Rotor-Craft Applications," NASA CR-165397, March 1981.

[12]Rogo, C., "Variable Area Radial Turbine Fabrication and Test Program," NASA CR-175091, Aug. 1986.

[13]Rogo, C., Hajek, T., and Chen, A. G., "Variable Stator Radial Turbine," NASA CR-174663, May 1984.

[14]Calvert, G. S., and Okapuu, U., "Design and Evaluation of a High-Temperature Radial Turbine—Phase I—Final Report," U. S. Army Aviation Material Lab., Fort Eustis, VA, USAAVLABS-TR-68-69, Jan. 1969.

[15]Calvert, G. S., and Okapuu, U., "Design and Experimental Evaluation of a High-Temperature Radial Turbine," U.S. Army Air Mobility Research and Development Lab., Moffett Field, CA, USAAMRDL-TR-71-20, May 1971.

[16]Vershure, R. W., Large, G. D., Meyer, L. J., and Lane, J. M., "A Cooled Laminated Radial Turbine Technology Demonstration," AIAA Paper 80-0300, Jan. 1980.

[17]Hammer, A. N., Aigret, G. G., Psichogios, T. P., and Rodgers, C., "Fabrication of a Cooled Radial Turbine Rotor," NASA CR-179503, June 1986.

[18]Lane, J. M., "Cooled Radial In-Flow Turbines for Advanced Gas Turbine Engines," American Society of Mechanical Engineers, New York, ASME Paper 81-GT-213,

[19]Large, G. D., and Myer, L. J., "Cooled Variable Area Radial Turbine Program," NASA CR-165408, Jan. 1982.

[20]Snyder, P. H., "Cooled High-Temperature Radial Turbine Program. I. First Turbine Design," NASA CR-179606, May 1987.